

Comparison between real-time auto-tuning PID and conventional PID controller for a dairy industrial evaporation process

MENG, Qingbo, ZHANG, Hongwei <<http://orcid.org/0000-0002-7718-021X>> and HOWARTH, Martin

Available from Sheffield Hallam University Research Archive (SHURA) at:

<https://shura.shu.ac.uk/31237/>

This document is the Accepted Version [AM]

Citation:

MENG, Qingbo, ZHANG, Hongwei and HOWARTH, Martin (2022). Comparison between real-time auto-tuning PID and conventional PID controller for a dairy industrial evaporation process. *International Journal of Modelling, Identification and Control*, 40 (1), 27-35. [Article]

Copyright and re-use policy

See <http://shura.shu.ac.uk/information.html>

Comparison between Real-Time Auto-Tuning PID and Conventional PID Controller for a Dairy Industrial Evaporation Process

Qingbo Meng

National Centre of Excellence for Food Engineering,
Sheffield Hallam University, United Kingdom
Email: mqb19861228@gmail.com

Hongwei Zhang*

Head of department, Engineering and Mathematics,
Sheffield Hallam University, United Kingdom
Email: h.zhang@shu.ac.uk

Martin Howarth

Director of the National Centre of Excellence for Food Engineering,
Sheffield Hallam University, United Kingdom
Email: engmho@exchange.shu.ac.uk

*Corresponding author

Abstract: Evaporation processes are commonly applied in the food industries to concentrate the liquor for future treatments. It presents challenges to the modelling and control approaches due to the system complexity, especially for the multi-effect evaporators. In this study, an industrial milk evaporation process is introduced and a mathematical model of a three-effect falling film evaporator is developed using MATLAB/SIMULINK with added disturbances. A real-time closed-loop auto-tuning PID and a conventional PID are both presented and applied to the model as the control strategies for the evaporation process. The simulation results are compared to illustrate the improvements from the auto-tuning PID controller.

Keywords: multi-effect falling-film evaporator, auto-tuning PID controller, industrial milk evaporation.

Biographical notes: Qingbo Meng received his MSc degree in Control Engineering from Coventry University, United Kingdom, in 2014. Qingbo Meng completed his Ph.D. in Control Engineering at Sheffield Hallam University in the United Kingdom in 2020. His research interests include complex system modelling, control, and advanced controllers' development.

Hongwei Zhang obtained his BEng degree in Automatic Control, MSc in Control Engineering and PhD in Aerospace Engineering all from Harbin Institute of Technology, China. Hongwei has also completed a PhD in Control Engineering at The University of Manchester in the UK. Hongwei is currently working as the Head of Department for Engineering and Mathematics at Sheffield Hallam University in the UK. His research interests are in the field of advanced control and condition monitoring of complex processes, industrial automation and robotics, and applications of artificial

intelligence.

Professor Martin Howarth has a PhD in Robotics from Nottingham Trent University and is a member of the Institution of Engineering and Technology (IET) and a Chartered Engineer. Martin Howarth is Director of the National Centre of Excellence for Food Engineering (NCFE). Over recent years, Martin has led and supported EU, EPSRC and Innovate UK projects and has contributed to the Knowledge Transfer Partnership programme within engineering at Sheffield Hallam University. Martin has authored and refereed technical publications in manufacturing, automation and robotics in a range of industrial sectors

This paper is a revised and expanded version of a conference paper entitled 'Performances Comparison between Real-Time Auto-Tuning PID and Conventional PID Controller for a Dairy Industrial Evaporation Process Control' presented at AICAE2019, Wuhan, China, 23-24 June 2019.

1 Introduction

Multi-effect falling film evaporators are widely used for the concentration of solutions in the dairy industry and are an energy-intensive process. It is normally applied as a part of the drying process to obtain many benefits for subsequent spray drying processes, including reducing the energy cost, improving the drying efficiency, and saving manufacturing time (Ruan et al., 2015). During an industrial evaporation process, the total solid content of the sterilised milk is normally designed to increase from approximately 5-10% to 45-55% at a temperature between 50-70°C under vacuum condition before feeding into the spray dryer.

However, literature on the modelling and control of multiple effects falling film evaporators for milk powder production are limited and the process has many challenges. These challenges include the non-linear and highly complex dynamic behaviour, difficult or even inability to measure the key variables during the real industrial manufacturing process. These all increase the difficulties of system modelling and controller development. Winchester and Marsh (1999)

developed a first-principle model of a falling film evaporator with mechanical vapour recompression to examine a three core control-loop. Runyon et al. (1991) presented a double effect evaporator to check the product output concentration consistency with multivariable controllers. Miranda and Simpson (2005) described a dynamic multiple-effect evaporation system model, determining that the most important parameters of the evaporation process are the global heat transfer coefficient and the latent heat of vaporization. More recently, two types of dynamic models named 'lumped' and 'distributed' were developed by Medhat et al. (2014) for an industrial multi-effect milk evaporation process.

As one of the classical control strategies, PID (Proportional-Integral-Derivative) based controllers have been extensively utilised in dairy manufacturing processes. Industrial applications can obtain many benefits from this strategy due to its low cost, relatively simple structures, easy to operate and available in most hardware and software (Bhat et al, 2020). Karimi and Jahanmiri (2006) described a two loop cascade control algorithm based on the PID control strategy

and applied it in a three effect falling film evaporator for the milk powder production process. Results showed that cascade control has a good performance on the disturbances rejection. A few years later, they improved the cascade control with triple loops for the same three effect falling film evaporators in 2009. Comparing with two loops cascade, the triple loop technique was shown to reduce the overshoot from 4.8% to 1.04%, and settling time from 505 to 287 seconds. There are also studies of PID type controllers developed to precisely control the specific evaporation process variables, such as temperature in the effect, product dry mass fraction and product flowrate (Winchester and Marsh, 1999); the water level in the steam generator, and the external steam amount supply (Cunningham et al., 2006); product flowrate through the process (Stapper, 1979).

Most of the previous studies in the evaporation process modelling and control field either focus on the reduction of energy consumption and system efficiency improvement (Zhang et al, 2018), or a new controller strategy development and specific parameters optimization to improve the system performance (Hu et al, 2019; Fang et al, 2019). In this paper, the authors present another perspective, which is comparing two PID based controllers to obtain their benefits and understand their limitations. It has contributions on the control techniques and selection for future research studies. In addition, the validation method in this paper compares the results and trends to similar studies conducted previously which could be used as a reference for the model based or less data referred research.

In this study, the three-effect falling film evaporator simulation model is developed by using MATLAB/Simulink and based on the Newell and Lee's evaporation model.

Meanwhile, a real-time auto-tuning PID is developed and the performance improvements are obtained comparing to conventional PID controllers.

2 Mathematical Formula and Modelling

2.1 Mass and Energy Balance

The basic requirement for the mathematical model is to replicate the actual process behaviours as accurately as possible in order to measure and control the system outputs in response to the various input and disturbance variables. The simulation model complies with the law of conservation of mass and energy through each part of the system no matter if the evaporator is a single or multi-effect. For a continuous evaporation process, the mass balance is represented by the following equations:

$$M_p = M_{in} - M_e \quad (1)$$

Where M_p , M_{in} and M_e present the mass flow of the liquid exiting, entering, and evaporated/removed from the evaporator. According to the Eq.1, the product concentration (total solid content) is calculated as below:

$$\omega_p = \frac{M_{in} \cdot \omega_f}{(M_{in} - M_e)} \quad (2)$$

Where, ω_p and ω_f are the product concentration of leaving from, and feeding into the evaporation system respectively. The heat energy balance is another priority principle that should be considered for the evaporation process. Based on the general energy balance equations given by Earle in 1983: Energy In = Energy Out + Energy Stored, the heat balance for the effect can be described as follows:

$$Q_1 = U_1 \cdot A_1 (T_s - T_1) = U_1 \cdot A_1 \cdot \Delta T_1 \quad (3)$$

Where,

Q_1 = Heat Transfer Rate of the effect.

U_1 = The overall heat transfer coefficient.

A_1 = Total Heat Transfer Surface Area.

T_s = Feed Steam Temperature to the effect.

T_1 = Boiling Temperature of the liquid.

ΔT_1 = Temperature Difference between the heating medium and the boiling liquid.

2.2 Effect sub-systems

A falling film evaporator effect normally contains a separator, a heat exchanger, a condenser, and a steam ejector.

(1). The separator, which separates the vapor and liquid phases when the evaporation process is taking place. The concentrated product forms a level at the bottom of the separator in order to avoid flow disturbances caused by the pump running dry. The Separator Level (L) is calculated by equation (4) as described by Newell & Lee (1989):

$$\frac{dL}{dt} = \frac{1}{\rho A} (F1 - F2 - F4) \quad (4)$$

Where ρ is the liquid density, A is the cross-sectional area of the separator, and $F1$, $F2$, & $F4$ are the feed, product, and vapor flowrates.

(2). The heat exchange occurs in the effect tubes, where the milk inside the tubes is heated by contacting the external hot steam over the tube walls, in the meantime, the film forms inside the surface of the tubes, and the water starts to be evaporated. Concentrated liquid drops down to the bottom of the effect then flows into the next effect and then to the spray dryer.

The concentration of the liquid is determined by equation (5) as follows:

$$\frac{dX2}{dt} = \frac{F1 * X1 - F2 * X2}{20} \quad (5)$$

Where $X1$ and $X2$ are the feed concentration and product concentration respectively.

(3). The condenser can remove the condensed vapor from the system.

(4). The steam ejector, which provides hot steam to heat the milk in the heat exchanger. The steam temperature (T_{steam}) is described by equation (6):

$$T_{steam} = 0.1538 * P_{steam} + 90 \quad (6)$$

Where, P_{steam} is the steam pressure. The mass and energy balances on both feed and steam ejector process in effect can be determined below according to the Eq.1, Eq.2, and Eq.3 listed above:

$$\frac{dM}{dt} = M_{in} - M_{out} - M_v \quad (7)$$

$$\frac{d(\rho_s V_s)}{dt} = \frac{\rho_s * M_{sin}}{v} - \frac{\rho_s * M_{sout}}{v} \quad (8)$$

$$\frac{dT}{dt} = M_f * (T_{in} - T_s) + C_p \Delta T * (T_{out} - T_s) \quad (9)$$

$$\frac{dH}{dt} = \frac{M_s}{V_s} * H1 + U * A * \Delta T * (T_s - T) - \frac{M_s}{V_s} * H0 * V * Q \quad (10)$$

2.3 System description and modelling

In this study, the sterilised milk feed concentration is 5% and the desired product concentration increases effect by effect to 30%, 38%, and finally to 52%. In a general dairy evaporation industry, the feed liquid product passes the pre-heater to reach the feed temperature before going into the first effect. However, the pre-heater sub-system is not included in this study and the feed temperature is set as a constant with disturbances.

The mathematical simulation model of the three-effect falling film evaporator is

developed using MATLAB/SIMULINK dynamic environment based on the mass and energy balance equations. The model contains three levels:

- i. The top-level shows the main inputs with added disturbances and mainly observed outputs of the simulation model.
- ii. The middle level describes how the three effect sub-systems and controller blocks are linked together and the information paths between them.
- iii. The lower level describes an example of the first effect sub-system which includes a heat exchanger, a steam ejector, a separator, and a condenser. The SIMULINK block 'GoTo' is applied to link effects together.

During the simulation process, the variable product flowrate is a manipulated variable to control the output product concentration. Further details and figures of the sub-systems are described in Appendix A.

2.4 Model validation

The purpose of model validation is to determine whether the model is an adequate representation of the physical process. In many practical situations, the accuracy to which the simulation model can imitate the physical process is the main consideration to evaluate if the model is good enough. However, it is impossible to obtain a perfect simulation model that can reproduce the entire industrial process without any errors.

The most common model validation method is by comparing the simulation results with the real manufacturing plant data. However, because the model developed in this study is an improvement from the model based on Newell and Lee's study, it is not mimicking a specific real industrial evaporation process.

So to obtain real plant data as a reference is impossible. Therefore, the validation process involves applying the inputs to the simulation model and comparing the trends and specific results with the previously published research work.

According to the main variables (flowrate, temperature, concentration) comparison with the previous study, most of the simulation results are within the acceptable range, and the figure trends are very similar and reasonable. It is believed that this model is accurate enough to achieve the process control objective and the controller improvement for the evaporation process. Details are listed in Appendix B.

3 Controller Development

3.1 Conventional PID controller

It is well known that the traditional PID is a widely used controller in many industrial applications to regulate temperature, flow, pressure, and other process variables. The following equation shows the mathematical function of the PID controller:

$$u(t) = K_p e(t) + K_i \int_0^t e(t') dt' + K_d \frac{de(t)}{dt} \quad (11)$$

where K_p , K_i and K_d are the coefficients for the proportional (P), integral (I), and derivative (D) terms respectively.

As a classic feedback control, the PID controller works by measuring the control variable, comparing it to a specific or desired value, known as set point, and applying the control law to determine the controller action that causes the control variable to track the set point. There are many methods to determine the value of the PID controller tuning parameters. In this study, the Ziegler-Nichols (ZN) 2nd tuning method is introduced to calculate the PID control gains.

3.2 Ziegler-Nichols (ZN) 2nd tuning methods

The second NZ method needs to find two values as well. A gain proportional K which makes the system in a steady-state oscillation condition and the system period P (see Fig.1). To find K , it normally starts with a closed-loop system and a lower or zero value of gain K . Increase the K value until a steady-state oscillation occurs.

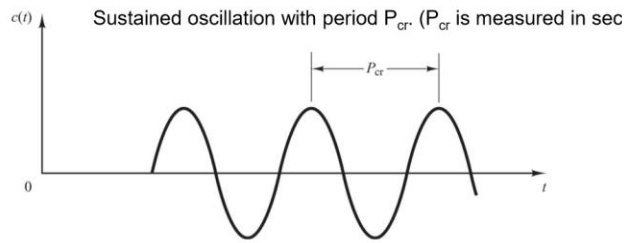


Figure 1. An example of steady-state oscillation

Once the K and P have been found from the curve, Table 1 is needed to calculate the PID control terms:

Table 1 ZN second tuning method gain estimator rules

Type of Controller	K_p	T_i	T_d
P	0.5K	∞	0
PI	0.45K	$P/1.2$	0
PID	0.6K	0.5P	0.125P

The control gain values recommended follow ZN's second method are in table 2 below:

Table 2. Gain values of each effect

	K_p	T_i

1 st effect	1.656	0.0417
2 nd effect	2.46	0.75
3 rd effect	1.72	0.54

3.3 Auto-tuning PID controller

The auto-tuning PID works by injecting a test signal to collect the system input and output data for estimating the frequency response. A MATLAB auto-tuner SIMULINK block is developed to do the plant frequency estimation in real-time base on the input-output data. The controller structure is below:

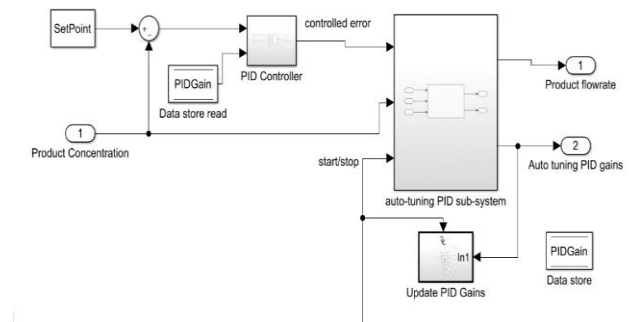


Figure 2. Auto-tuning PID control structure

The auto-tuning process works in two steps:

1. When the auto-tuning process starts, a test signal is injected into the auto-tuner block as an input to the plant system. After that, the plant output data is collected and stored via the auto-tuner. This series of input-output data is used to estimate the system frequency response in real-time. Once the tuning ends, the PID gains are computed based on the estimated system frequency.
2. The new gain values are transferred to the PID controller, re-writing the old PID gain values to complete the auto-tuning process.

Subsequently the auto-tuner block stops tuning and the system control is transferred to the new, updated PID controller.

This is an online tuning process, and the tuning algorithm aims to balance system performance and robustness while achieving the specific control target. Consequently it can find more appropriate PID gains for the plant system compared with manual calculating methods.

It is clear that finding a better gain also depends on the start-stop duration. Basically, a more complex system needs a longer auto-tuning period to obtain more accurate gains. However, compromise on system accuracy in order to save tuning time is also sometimes necessary.

4. Simulation Result and Comparison

4.1 Auto-tuning period

As discussed above, five different tuning durations of 30, 90, 180, 240, 480 seconds, are used to indicate the most suitable auto-tuning time for the three effects in this model. The following two figures show the product concentration leaving the 1st and 2nd effects with 30 and 480 auto-tuning time.

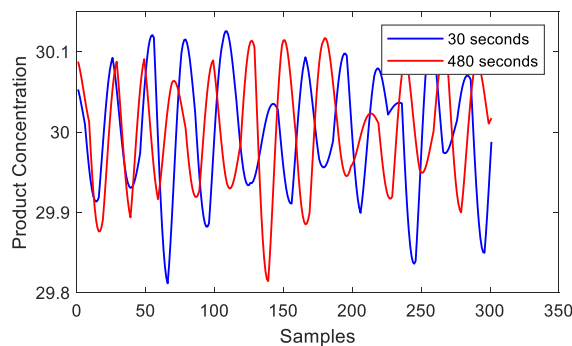


Figure 3. 1st effect product concentration with 30 and 480 auto-tuning period

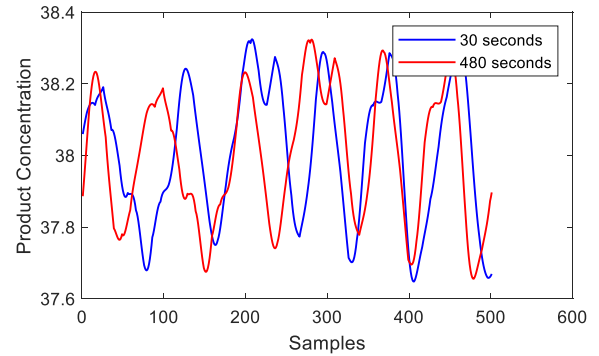


Figure 4. 2nd effect product concentration with 30 and 480 auto-tuning period

According to the two figures above, the product concentration trend and amplitude of the 1st and 2nd effects are very similar in both 30 and 480 seconds. No obvious improvements are obtained with increasing auto-tuning time from 30 to 480 seconds, which indicates that 30 seconds is sufficient to find the appropriate controller gains for the 1st and 2nd effect.

However, for the 3rd effect, different auto-tuning time results in different control performances:

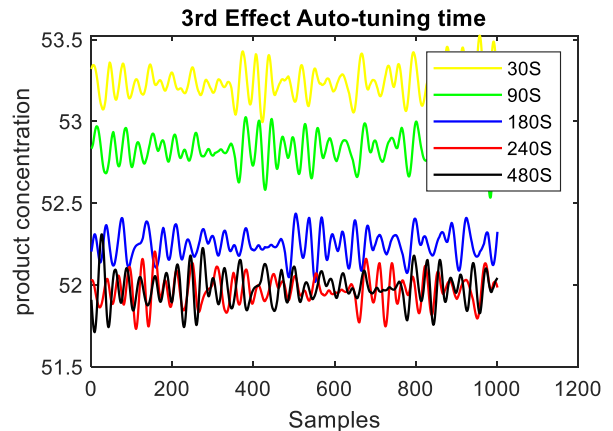


Figure 5. 3rd effect product concentration with different tuning time

It is evident from Fig.5 that with the increasing of tuning time, the 3rd effect product concentration is moving closer and

closer to the designed target (52%). In addition, the system performances in 240 and 480 seconds auto-tuning time are almost the same, which means that a minimum of 240 seconds is required for the 3rd effect to find the PID gains.

4.2 Results comparison

It is assumed that the auto-tuning PID should have a better performance than the conventional PID controller. Because the conventional PID control gain values are decided by the manual calculation based on the theoretical system transfer function. However, almost all of the industrial manufacturing processes are highly complex non-linear systems. To obtain these transfer functions are difficult and are not precise enough to describe the nonlinear systems.

The following three figures show the results comparison and proof of the assumption.

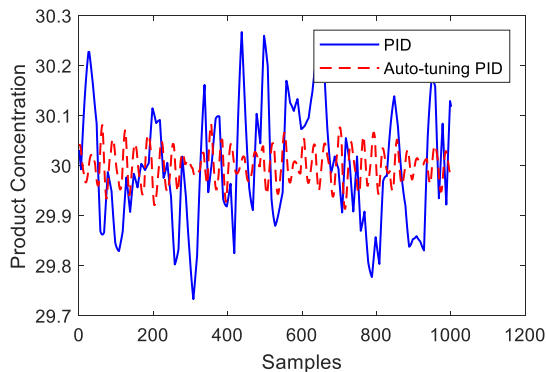


Figure 6. 1st effect product concentration

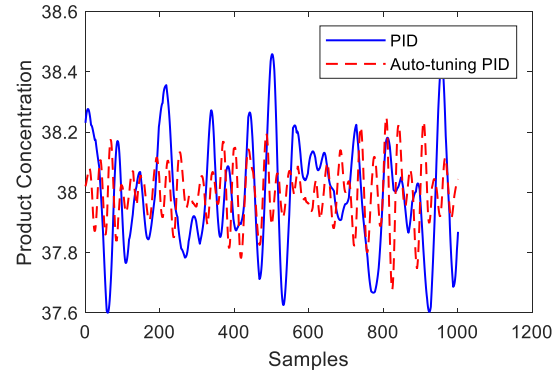


Figure 7. 2nd effect product concentration

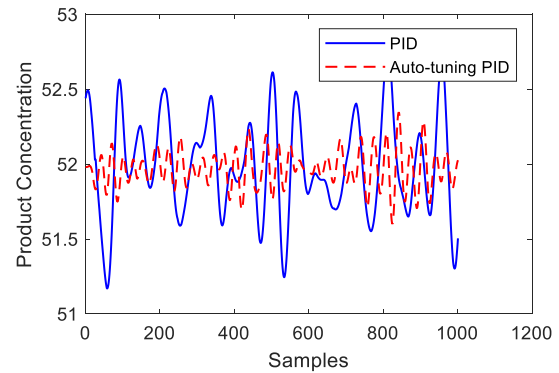


Figure 8. 3rd effect product concentration

Both control strategies can achieve the control targets to maintain the product concentration of each effect within an acceptable vibration range close to the desire set-point. However, it is clear from the comparison results that the auto-tuning PID has better performance on accuracy control and maintaining system stability.

Table 3. Variance values of each effect concentration output

	PID	Auto-tuning
Effect 1	0.057	0.021
Effect 2	0.185	0.015
Effect 3	0.330	0.025

The increasing variance values (shown in Table 3) controlled by conventional PID show that the more complex the plant is or the more effects the plant contains, the more difficult it is for the conventional PID to maintain the system performances. On the contrary, the variance values controlled by auto-tuning PID are changing within a very limited range, which means that the auto-tuning PID is more suitable than a conventional PID controller for a complex system.

5. Conclusions and Future Works

One major result from this study was that the auto-tuning PID has smaller errors than the conventional PID on the product concentration control. This means the proportional and integral gains computed by the online auto-tuner based on the system input/output data can achieve more precious control results than the gains calculated by the Ziegler–Nichols method.

However, one of the disadvantages of the auto-tuning method is the tuning time required to obtain the input/output data. For the evaporation process in this study, at least 240 seconds of tuning time is necessary to find the appropriate PID gains automatically. This period could vary in different simulation processes.

For future works, one can focus on the more advanced controller development to seek benefits comparing to the PID based controllers. Although the auto-tuning PID performs a little bit better than the conventional PID in this paper, it is still a PID based control strategy essentially. As discussed above, the results were improved, but not very much. Other future works can be done to complete the whole system model by adding pre-heater and spray dryer subsystems to the evaporation process.

References

- Ruan, Q., Jiang, H., Nian, M., and Yan, Z. (2015). Mathematical modeling and simulation of countercurrent multiple-effect evaporation for fruit juice concentration, *Journal of Food Engineering*, 146, pp.243-251.
- Winchester, J.A. and Marsh, C. (1999). Dynamics and control of falling film evaporators with mechanical vapor recompression, *Chemical Engineering*, 77, pp.357-371.
- Runyon, C.H., Rumsey, T.R. and McCarthy, K.L. (1991). Dynamic simulation of a non-linear model of a double effect evaporator, *Journal of Food Engineering*, 14, pp.185-201.
- Miranda, V. and Simpson, R. (2005). Modelling and simulation of an industrial multiple effect evaporator: tomato concentrate, *Journal of Food Engineering*, 66, pp.203-210.
- Medhat, B., Fanaei, M.A. and Zohreie, H. (2014). Mathematical modelling and dynamic simulation of multi-effect falling-film evaporator for milk powder production, *Mathematical and Computer Modelling of Dynamical Systems*, 21, pp.1-23.
- Karimi, M. and Jahanmiri, A. (2006). Nonlinear Modeling and Cascade Control Design for Multi Effect Falling Film Evaporators, *Iranian Journal of Chemical Engineering*, 3, pp.52-63.
- Newell, R.B. and Lee, P.L. (1989). *Applied Process Control: A Case Study*, New York: Prentice-Hall.
- Cunningham, P., Canty, N., O'Mahony, T., O'Connor, B. and O'Callaghan, D. (2006). System Identification of a

Falling-film Evaporator in the Dairy Industry, in *Proceedings of the UK Automatic Control Conference*, Sheffield.

Stapper, H.L. (1979). Control of an evaporator and spray dryer using feedback and ratio feedforward controller, *Journal of Dairy Science Technology*, 14, pp.241-257.

Zhang, X., Meng, C., Quan, S., and Shen, S. (2018). A numerical investigation of liquid film flow and film thickness distribution outside a horizontal tube, *International Journal of Low-Carbon Technol*, 13, pp. 424-431.

Hu, B., Yan, H., and Wang, R. (2019). Modelling and simulation of falling film evaporator for a water vapor heat pump system, *Applied Energy*, 255.

Fang, J., Li, K., and Diao, M. (2019). Establishment of the falling film evaporation model and correlation of the overall heat transfer coefficient, *Royal Society Open Science*, 6: 190135.

Bhat, V.S., Bhat, S., and Gijo, E.V. (2020). Robust design of proportional integral controllers: a Taguchi-grey approach. *International Journal of Modelling, Identification and Control*, 35:4, pp. 363-375.

Appendix A

The SIMULINK block diagrams in the following figures show the details of how the effects, controller and inputs linked together in the MATLAB dynamic environment. There are three levels of the evaporator SIMULINK model.

- i. The top level (Figure A-1) shows the main inputs and outputs of the simulation model.
- ii. The middle level (Figure A-2) is where the main structure of the model can be observed. It shows how the three effects, controller blocks, and inputs with disturbances linked together and the information paths between them.
- iii. The lower level (Figure A-3 and A-4) is an example of the first effect system which shows how the heat exchanger, steam ejector, separator and condenser linked together.

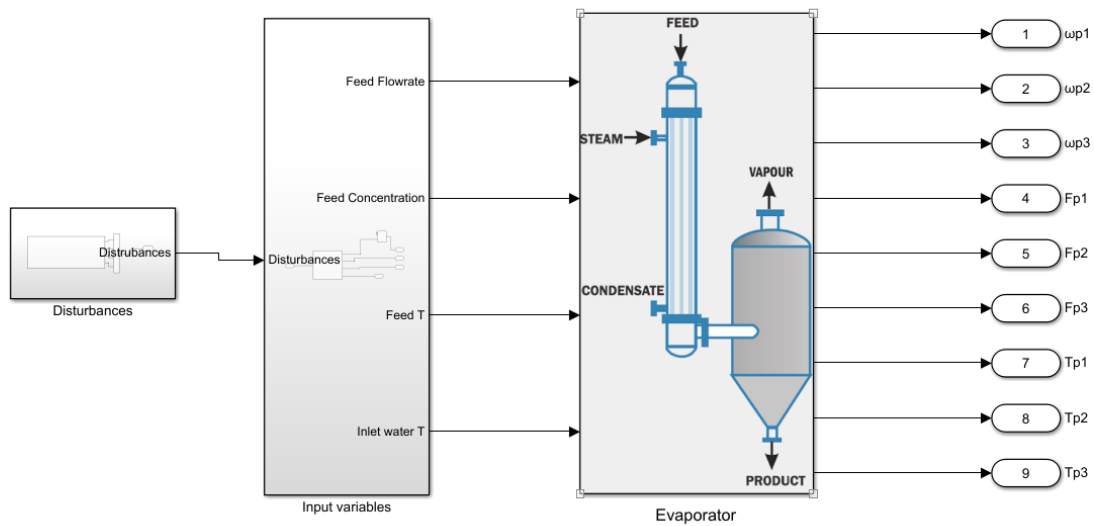


Figure A-1. Top level of evaporator SIMULINK block diagram

The four main inputs variables with disturbances have been shown at the top level of the simulation block. The three effects and controller blocks are developed as sub-systems under the evaporator block. The right-hand side in figure A-1 is the mainly observed outputs, which are the product concentration, flowrate, and temperature of the three different effects.

Comparison between Real-Time Auto-Tuning PID and Conventional PID Controller for a Dairy Industrial Evaporation Process

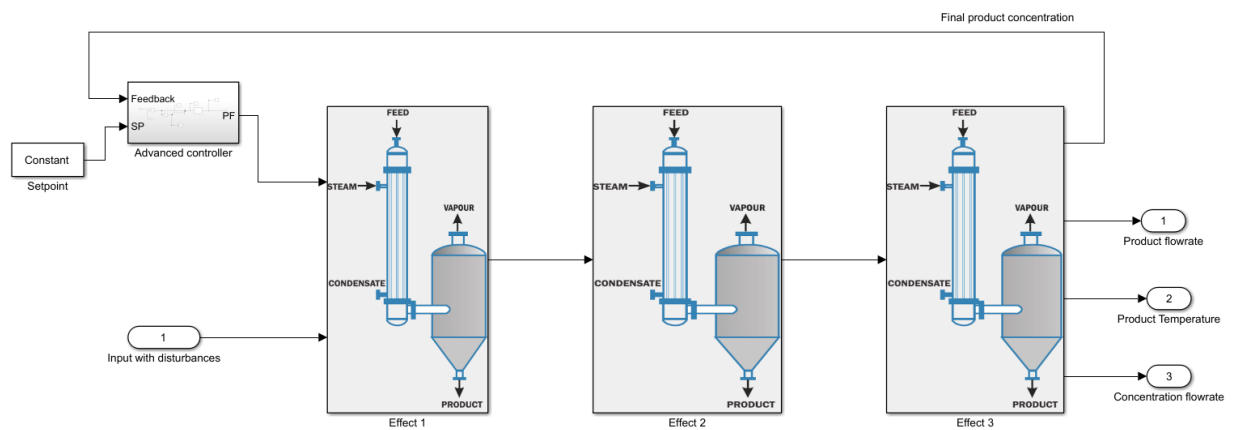


Figure A-2. Middle level SIMULINK diagram of three effect falling-film evaporator

Figure A-2 includes three effects blocks and a controller block. The advanced controller block is an outer-loop controller. There is one basic PID controller under each effect block. Meanwhile, there are many 'From' and 'GoTo' SIMULINK blocks under each effect to link them together.

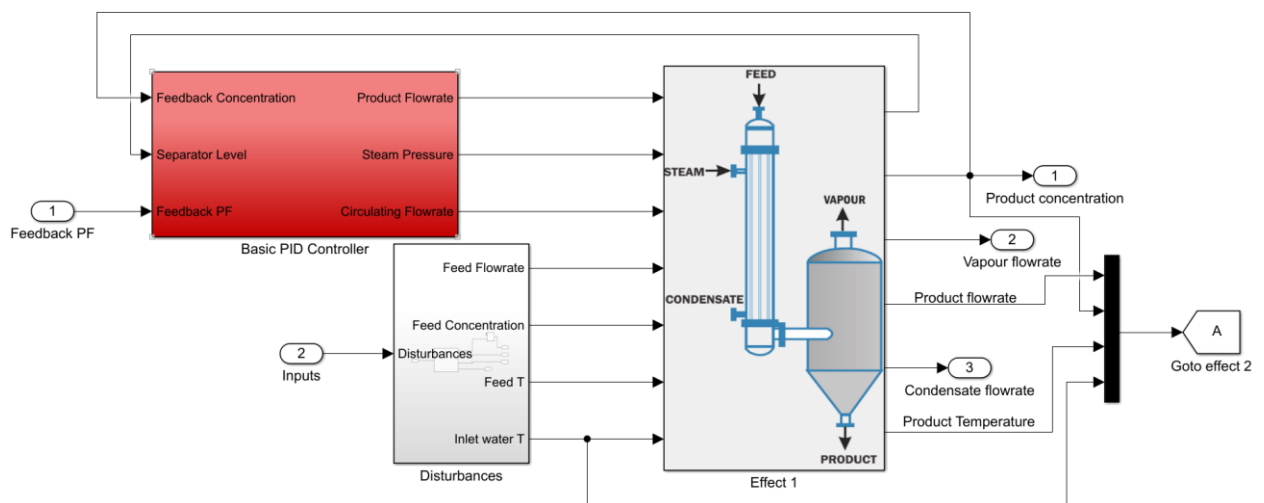


Figure A-3. An example of lower level effect SIMULINK diagram

Comparison between Real-Time Auto-Tuning PID and Conventional PID Controller for a Dairy Industrial Evaporation Process

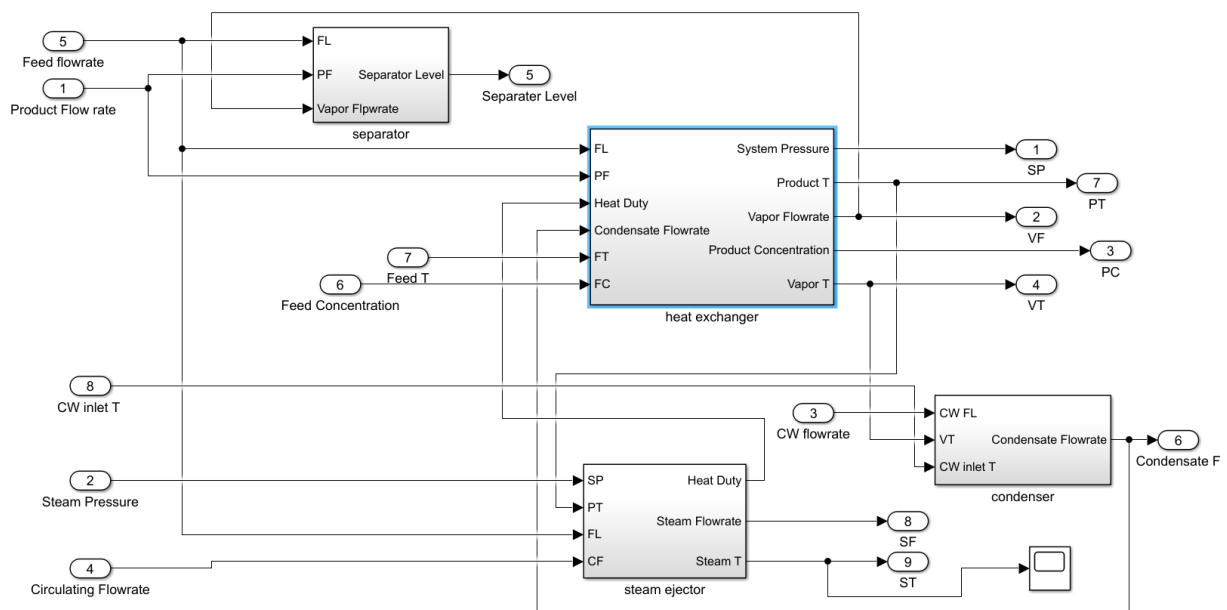


Figure A-4 Falling film evaporator effect sub-system block

Figure A-3 and A-4 has indicated the arrangement of inputs and outputs to the first effect. Four output variables from the first effect are treated as inputs to the second effect. The SIMULINK block 'GoTo' is developed to link effects together. Product flowrate is a manipulated variable to control the product concentration under the basic PID controller block.

Appendix B

The designed simulation value of product concentration in each effect is 30%, 38%, and 52%. The study of a similar three effect falling film evaporator is published by Farsi and Jahanmiri in 2009. They indicated that the designed product concentration increases from 8.5% to 48%. The details are listed in Table B-1

Table B-1. Designed product concentration in each effect of two studies

	Product Concentration	
	Farsi 2009	This study
Feed	8.5%	5%
Effect-1	13.35%	30%
Effect-2	29.56%	38%
Effect-3	48%	52%

From the table above, both studies are aiming to increase the product concentration effect by effect to reach the desired control targets. The difference between them is the concentration gaps between effects. The biggest gap of concentration increasing in Farsi's study is from effect 2 to effect 3, which is approximately 19%. However, the value from this paper is exact 25% from the first effect to the second one. Another difference is the total concentration increased range which is 39.5% and 47% respectively. Because the targets of both studies are similar, the process parameters trend should be relatively similar as well.

The following two figures show the trend of the product concentration for both studies. Farsi's study just published the data of the third effect with 10% step input disturbances (Fig B-1(a)). It is indicated that the two figures have a very similar trend of product concentration from a lower value to a target set-point.

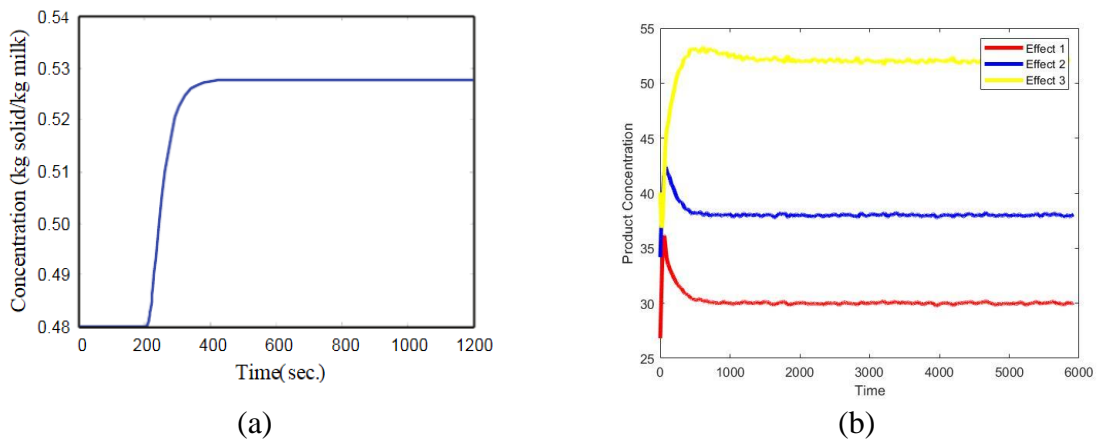


Figure B-1 Product concentration simulation results for both studies

However, due to the different scales of the two studies and the concentration gaps between effects, the process parameters are likely to be varied. The following table B-2 shows the product feed flowrate and the flowrate in effects. The units of flowrate are not the same for both, which Farsi's is in kg/hr and this study is in kg/min. In order to make the comparison easier to distinguish, the kg/min is transformed into kg/hr.

Table B-2 Flowrate variables in each effect for both studies

	Flowrate steady-state values of each effect (kg/hr)	
	Farsi 2009	This study
Feed	10000	600
Effect-1	6367.0	400
Effect-2	2875.5	219
Effect-3	1770.0	61.9

It has been generally accepted that the higher concentration the material is, the slower it flows in the evaporator. And the simulated product concentration increased from effect to effect are different. It is reasonable to assume that the flowrates in the evaporation process have a proportional correlation. The table above can be re-calculated as:

Table B-3 Re-calculated flowrate variables values

	Flowrate steady-state values of each effect (kg/hr)	
	Farsi 2009	This study
Feed	1	1
Effect-1	0.6367	0.667
Effect-2	0.2875	0.365
Effect-3	0.177	0.103

It is obvious that with the same feed flowrate, the product flowrate in each effect has a similar trend of the two studies. The following figure B-2 shows the trend.

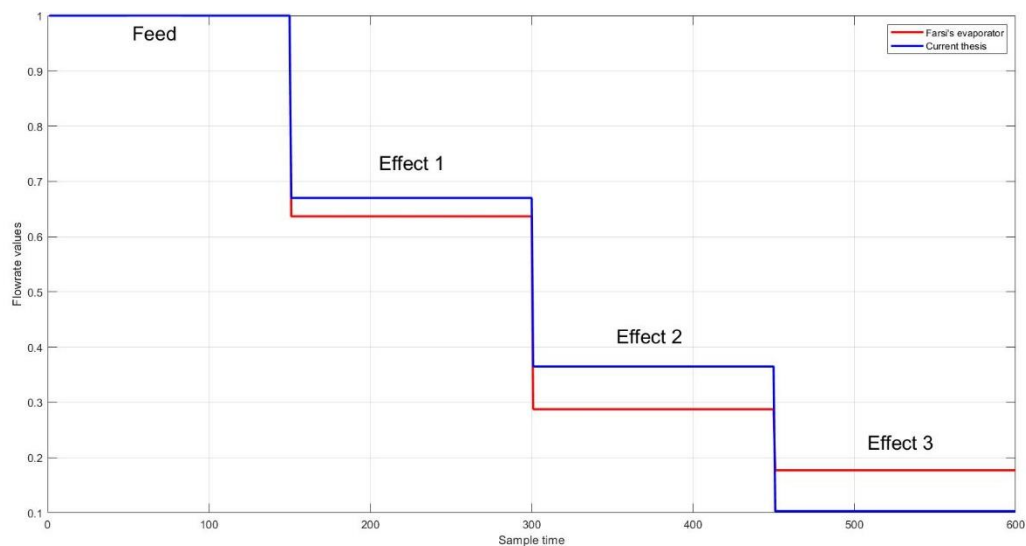


Figure B-2 Flowrate trend of both evaporation process

Another important variable is the product temperature in the effect. In the industrial manufacturing evaporation process, the product temperature normally decreases progressively from effect to effect. In Farsi's paper, the three effects product temperature values are 72°C, 58°C and 45°C from the first to the third respectively. The values of current

model simulation results are 88.86°C, 53.27°C and 44.38°C respectively as shown in Table B-4.

Farsi's model contains 4 pre-heater system to heat the raw milk until 72°C before feeding into the first effect. Meanwhile, there is an assumption that the heat loss between the pre-heater and the first effect system is neglected. That results in the product temperature of the feed and the first effect are both 72°C. With the water removed from the milk, the product temperature drops from 72°C to 45°C finally when leaving the evaporator.

Table B-4 Product temperature of each effect of Farsi's research and this study

	Product temperature steady-state values of each effect (°C)	
	Farsi 2009	This study
Feed	72	40
Effect-1	72	88.86
Effect-2	58	53.27
Effect-3	45	44.38

Unlike Farsi's model, the pre-heater system was not developed and applied in the simulation model in this paper. The feed temperature is designed to be 40°C with disturbances. The concentration increasing gap between first and second effect is larger than Farsi's model, which means more water need to be evaporated in the first effect. So the higher product temperature is a reasonable value. Comparing the second and third effects, both studies have similar values.

According to the main variables (flowrate, temperature, concentration) comparison with the previous study, most of the simulation data is within an acceptable range, and the figure trends are very similar and reasonable. It is believed that this model is accuracy enough to achieve process control comparison and the controller improvement for the evaporation process.